

RESEARCH ARTICLE

Ezh2 represses the basal cell lineage during lung endoderm development

Melinda E. Snitow¹, Shanru Li^{2,3}, Michael P. Morley^{2,3}, Komal Rathi^{2,3}, Min Min Lu^{2,3}, Rachel S. Kadzik^{2,3}, Kathleen M. Stewart^{2,3} and Edward E. Morrisey^{1,2,3,4,*}

ABSTRACT

The development of the lung epithelium is regulated in a stepwise fashion to generate numerous differentiated and stem cell lineages in the adult lung. How these different lineages are generated in a spatially and temporally restricted fashion remains poorly understood, although epigenetic regulation probably plays an important role. We show that the Polycomb repressive complex 2 component Ezh2 is highly expressed in early lung development but is gradually downregulated by late gestation. Deletion of Ezh2 in early lung endoderm progenitors leads to the ectopic and premature appearance of Trp63⁺ basal cells that extend the entire length of the airway. Loss of Ezh2 also leads to reduced secretory cell differentiation. In their place, morphologically similar cells develop that express a subset of basal cell genes, including keratin 5, but no longer express high levels of either Trp63 or of standard secretory cell markers. This suggests that Ezh2 regulates the phenotypic switch between basal cells and secretory cells. Together, these findings show that Ezh2 restricts the basal cell lineage during normal lung endoderm development to allow the proper patterning of epithelial lineages during lung formation.

KEY WORDS: Basal cell, Endoderm, Lung, Mouse

INTRODUCTION

The lung epithelium is derived from a small population of ventral anterior foregut endoderm that expresses the transcription factor Nkx2-1 (Herriges and Morrisey, 2014). This region of the foregut is polarized, such that the ventral region contains the lung endoderm progenitors and expresses high levels of Nkx2-1, whereas the dorsal region does not express Nkx2-1 but rather expresses high levels of the transcription factors Sox2 and Trp63. As development progresses, the primitive lung endoderm is patterned along its anterior-posterior axis, resulting in distinct epithelial cell lineages in the mature airways and in gas exchange alveolar regions. Each of these lineages is regulated in a tightly controlled spatial and temporal manner, resulting in the appropriate deposition of epithelium in regions where they are uniquely required, such as alveolar type 2 cells in the distal alveolus, and basal and secretory cells in the airways.

Several signaling and transcriptional regulators have been shown to play important roles in regulating lung epithelial development,

including Gata6, Nkx2-1, Sox2 and Sox9 (Kimura et al., 1996; Liu et al., 2002; Yang et al., 2002; Que et al., 2007, 2009; Tompkins et al., 2011; Rockich et al., 2013). In addition to these regulators, recent evidence has pointed to an important role for epigenetic chromatin modifiers in specification and differentiation of various lung endoderm lineages, including early stem/progenitor populations. Hdac1 and Hdac2 are essential for the development of Sox2⁺ proximal endoderm progenitors, which generate all of the epithelial lineages lining the large airways, including secretory, ciliated and basal cell lineages (Wang et al., 2013). Hdac1/2 regulate Sox2 expression and proliferation of Sox2⁺ endoderm progenitors by repressing Bmp4 signaling as well as the cell cycle inhibitors p16 (Cdkn2a – Mouse Genome Informatics), p21 (Cdkn1a – Mouse Genome Informatics) and Rb1 (Wang et al., 2013). However, which role other chromatin remodeling complexes play during lung epithelial patterning and development remains poorly understood.

In this report, we show that Ezh2, a crucial component of the Polycomb repressive complex 2 (PRC2), is required to silence the basal cell lineage during lung development. In the absence of Ezh2, Trp63 expression is initiated early in lung epithelial development, and Trp63⁺ cells become basally localized and subsequently express additional markers of the basal lineage, including keratin 5 (Krt5) and keratin 14 (Krt14). These Trp63⁺ basal cells extend the full length of the Sox2⁺ conducting airway epithelium, which resembles the patterning of this lineage in human but not in mouse lung airways. The ectopic appearance of basal cells is accompanied by a severe depletion of mature secretory cells, a lineage that can interconvert with basal cells in the adult respiratory airways (Tata et al., 2013). Instead of mature secretory cells, Trp63⁺/Krt5⁺ cells develop, which are morphologically similar to secretory cells and occupy their niche, but do not express high levels of secretory lineage genes such as *Scgb1a1*. These data indicate that Ezh2/PRC2 is required to restrict the basal cell lineage during lung development to allow for the proper differentiation of the secretory cell lineage.

RESULTS

Ezh2 is broadly expressed in the lung during development

Examination of RNA-seq data from embryonic day (E) 12.5 and adult mouse lungs that we have recently published (Herriges et al., 2014) shows that Ezh2 is expressed at high levels at E12.5 but is significantly downregulated in the adult lung (Fig. 1A). To better define the expression pattern of Ezh2 during lung development, we performed immunohistochemistry (IHC) for Ezh2 at various stages of mouse lung development. Ezh2 is ubiquitously expressed in the respiratory endoderm and lung mesoderm early in development, including in regions containing Sox2 and Sox9 endoderm progenitors (Fig. 1B; supplementary material Fig. S1A). As development progresses, Ezh2 expression decreases in overall levels (Fig. 1B; supplementary material Fig. S1A,B). These data

¹Department of Cell and Developmental Biology, University of Pennsylvania, Philadelphia, PA 19104, USA. ²Department of Medicine, University of Pennsylvania, Philadelphia, PA 19104, USA. ³Cardiovascular Institute, University of Pennsylvania, Philadelphia, PA 19104, USA. ⁴Institute for Regenerative Medicine, University of Pennsylvania, Philadelphia, PA 19104, USA.

*Author for correspondence (emorris@med.upenn.edu)

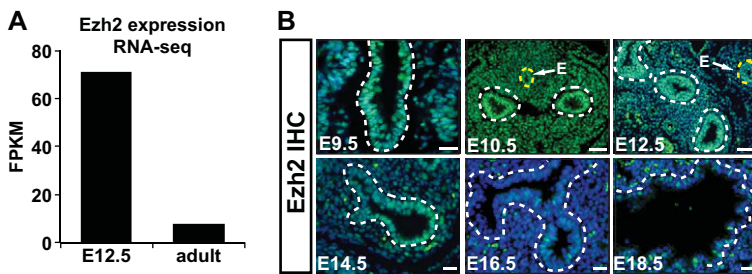


Fig. 1. Expression of Ezh2 during lung development. (A) RNA-seq data showing fragments per kilobase of transcript per million mapped reads (FPKM) for Ezh2 in E12.5 and adult lungs. (B) IHC for Ezh2 during different stages of lung development. White dashed outlines show separation between developing lung endoderm and surrounding mesoderm. Yellow dashed line highlights the esophagus (E). Note the decrease in Ezh2 expression in both the endoderm and mesoderm as development progresses. Scale bars: 20 µm in E9.5, E14.5-E18.5; 50 µm in E10.5 and E12.5.

suggest that Ezh2, and PRC2 in general, plays an important role in early lung endoderm development.

Loss of Ezh2 expression in the developing lung endoderm results in impaired epithelial development

To functionally assess the role of Ezh2 during mouse lung endoderm development, we generated a lung endoderm-specific loss-of-function mutant by crossing *Ezh2^{lox/lox}* mice with the early lung endoderm recombinase *Shh^{cre}* (Harfe et al., 2004; Wang et al., 2013). As *Shh^{cre}:Ezh2^{lox/lox}* mutants do not survive after birth (data not shown), we assessed lung development at E18.5. *Shh^{cre}:Ezh2^{lox/lox}* mutant lungs were often smaller than their control littermates (Fig. 2A). IHC and quantitative real-time PCR (qPCR) revealed a marked decrease in expression of genes associated with the secretory lineage, including *Scgb1a1*, *Scgb3a2* and SSEA1 (*Fut4* – Mouse Genome Informatics) (Fig. 2B–E) (Xing et al., 2010). By contrast, we did not observe decreased expression, either by IHC or by qPCR, of markers of the ciliated epithelial lineage

such as *Tubb4* (Fig. 2B,F). These data suggest a loss of secretory cell differentiation in *Shh^{cre}:Ezh2^{lox/lox}* mutant lungs.

Loss of Ezh2 leads to the development of ectopic Trp63+ basal cells

To better define the alterations caused by the early loss of Ezh2 expression in the developing lung endoderm, we performed transcriptome analysis at E14.5 in *Shh^{cre}:Ezh2^{lox/lox}* mutants and *Shh^{cre}* controls using microarray analysis. The E14.5 time point was used in these assays, as this allows for complete deletion of genes using the *Shh^{cre}* driver (Wang et al., 2013). In total, 188 genes were upregulated and 86 genes were downregulated more than 1.25-fold in *Shh^{cre}:Ezh2^{lox/lox}* mutant lungs at E14.5 (supplementary material Table S1). A gene ontology (GO) analysis using the Database for Annotation, Visualization and Integrated Discovery (DAVID) indicates that a broad array of developmentally regulated genes is deregulated by loss of Ezh2. Within the top three enriched GO categories (Table 1), we found the transcription factor Trp63,

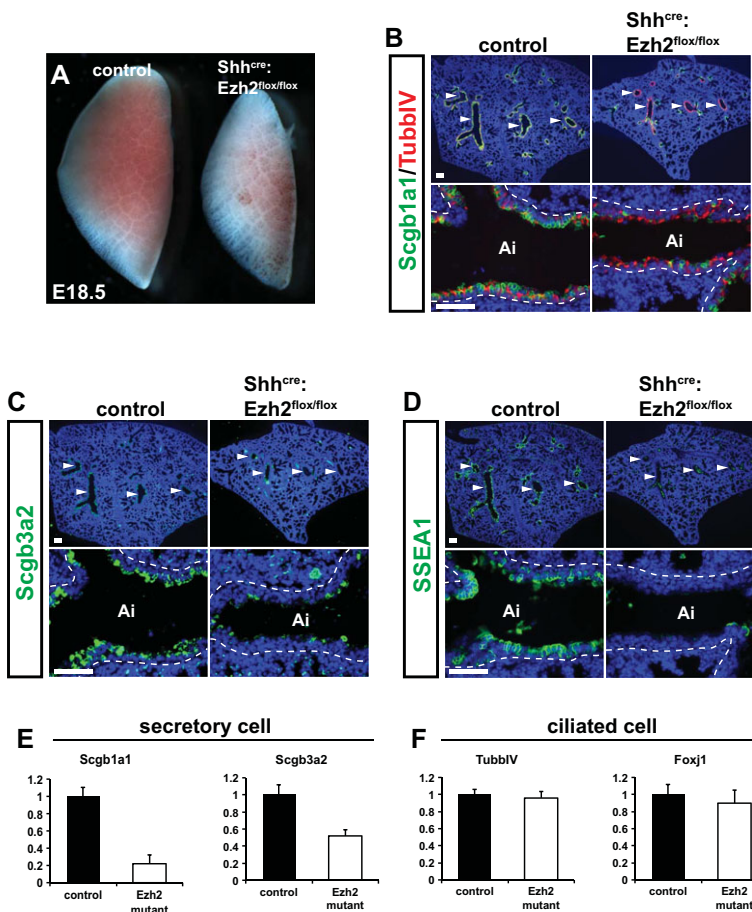


Fig. 2. Loss of Ezh2 in the developing lung endoderm leads to reduced secretory cell differentiation. (A) *Shh^{cre}:Ezh2^{lox/lox}* mutant lungs appear smaller than their control littermates at E18.5. (B) IHC for Scgb1a1 and Tubb4V reveals decreased Scgb1a1+ secretory cells in *Shh^{cre}:Ezh2^{lox/lox}* mutant lungs at E18.5. (C) Scgb3a2 IHC shows reduced expression and thus reduced secretory cell differentiation in *Shh^{cre}:Ezh2^{lox/lox}* mutant lungs. (D) SSEA1 IHC shows reduced expression and thus reduced secretory cell differentiation in *Shh^{cre}:Ezh2^{lox/lox}* mutant lungs. Arrowheads indicate comparable airways between control and mutant lungs; dashed lines outline airway epithelium; Ai, airways. Scale bars: 50 µm. (E,F) qPCR for secretory and ciliated epithelial lineages in control and *Shh^{cre}:Ezh2^{lox/lox}* mutant lungs at E18.5.

Table 1. DAVID/GO analysis of microarray data from E14.5 *Shh^{cre}* control and *Shh^{cre}:Ezh2^{fllox/fllox}* mutant lungs shows that Trp63 expression is found in the top three categories identified, which includes genes related to development

Cluster #	Cluster description	Enrichment score	FDR <i>P</i> value	Fold enrichment
Cluster 1	Homeobox, TF activity, Developmental protein, Regionalization, Anterior/posterior pattern formation Skeletal system development, Embryonic morphogenesis, Positive regulation of biosynthetic process Embryonic organ and skeletal system development & morphogenesis, Chordate embryonic development Pou3f3, Tgfb2, Eya4, Lin28b, Alx1, Hoxb13, Hoxb9, Hoxb7, Hoxb6, Ccng1, Krt17, Meox1, Pax9, Lpin1, Jag2, Isl1, Anxa11, Rec8, Hoxc10, Hoxc9, Hoxc6, Hoxc4, Trp63, Fgf12, Runx1, Cdkn1a, Pax2, Ovol1, Anxa1, Dkk1, Sp9, Eya2, Meis2, Zfx4, S100a6, Notch2, Tbx15, Psrc1, Lef1, Zmat3, Trp53inp1, Bmp8b, Cdkn2a, Trnp1, Grhl3, En2, Hoxa1, Hoxa10, Cebpa, Pcsk6, Utf1, Dbx1, Ebf3, Cacna1a, Nrg1, Mapkapk3, Eda2r	5.424	7.35E-09	9.6
Cluster 2	Embryonic limb/appendage development & morphogenesis Proximal/distal pattern formation Alx1, Hoxb7, Hoxb6, Jag2, Hoxc10, Hoxc9, Hoxc4, Trp63, Pax2, Dkk1, Notch2, Tbx15, Lef1, Hoxa1, Hoxa10	3.346	0.0079	4.54
Cluster 3	Regulation of cell growth & size, Epidermis development, Ectoderm development Positive regulation of developmental process, Positive regulation of multicellular organismal process Tgfb2, Hoxb13, Krt17, Scin, Htr2a, Trp63, Runx1, Ovol1, Notch2, Psrc1, Zmat3, Cdkn2a, Grhl3, Cacna1a, Nrg1	2.163	0.093	8.05

which is a marker of the basal cell lineage in the trachea (Rock et al., 2009). Jag2 and Itgb4, two other respiratory basal cell-specific genes, were also upregulated in the microarrays (Table 2; supplementary material Table S1). Several keratins, including Krt4/15/17, that are associated with Trp63-expressing squamous cell carcinomas (Blobel et al., 1984), were upregulated in the microarray (Table 2). Previously published microarray data comparing tracheal basal cells with surrounding epithelium (Rock et al., 2009) were re-analyzed, and 25.5% (48/188) of the genes upregulated in *Shh^{cre}:Ezh2^{fllox/fllox}* mutant lungs overlapped with the adult tracheal basal cell signature (Fig. 3A). Basal cells are a stem cell population that exists in the basal surface of the trachea and proximal main stem bronchi of the rodent lung (Rock et al., 2009, 2010). Basal cells do not normally develop in the mouse trachea and lung bronchi until just before birth (~E18.5), and are not found in large quantities until the lung is fully mature. The increase in Trp63 expression indicated that either this transcription factor was upregulated throughout the developing lung epithelium or that basal cells were ectopically developing at a much earlier time and in a much greater number than is normally found in the mouse lung.

qPCR confirmed upregulation of Trp63 in *Shh^{cre}:Ezh2^{fllox/fllox}* mutant lungs at E14.5 (Fig. 3B). Moreover, qPCR showed that *Shh^{cre}:Ezh2^{fllox/fllox}* mutant lungs expressed the carboxy-terminal alpha isoform, which is associated with basal cells [Fig. 3B;

Signoretti et al. (2000)]. IHC analysis shows extensive Trp63+ cells lining the entire airways of *Shh^{cre}:Ezh2^{fllox/fllox}* mutant lungs at E14.5, whereas control lungs had few, if any, of these cells (Fig. 3C). Of note, Trp63+ cells were found along the entire length of the airway tree all the way up to the bronchioalveolar junction but not into the alveolar region. Together, these data demonstrate an expansion of the Trp63+ basal cell lineage in the lungs of *Shh^{cre}:Ezh2^{fllox/fllox}* mutants.

Examination of distal epithelial gene expression revealed little change in most markers of these cells, including Sftpc, Sftpb and Aqp5 (supplementary material Fig. S2A,B). However, the microarray data did reveal increased expression of several cyclin-dependent kinase inhibitors, as well as alterations in signaling pathways, such as Shh, Dkk1, Lef1 and Tgfb2 (supplementary material Fig. S2C-E). Interestingly, we observed ectopic expression of Pax2 in the distal epithelium in mutant lungs by microarray, *in situ* hybridization and qPCR (supplementary material Fig. S2C,D,G). Moreover, Pou3f3/Bm1, a direct target of Pax2, was also upregulated in *Shh^{cre}:Ezh2^{fllox/fllox}* mutant lungs (supplementary material Fig. S2C,G). Chromatin immunoprecipitation (ChIP) assays for the Ezh2-deposited chromatin mark H3K27me3 revealed a strong association of this mark with the Pax2 promoter in wild-type lungs, indicating that Pax2 is a direct target of Ezh2/PRC2 repression (supplementary material Fig. S2F). These data suggest that de-repression and ectopic expression of exogenous transcription factors in the distal epithelium disrupts normal gene expression patterns and inhibits proper distal epithelial development in *Shh^{cre}:Ezh2^{fllox/fllox}* mutant lungs.

Table 2. Genes associated with Trp63-expressing basal cells or squamous cell carcinomas are found to be upregulated in the microarray analysis

Symbol	Fold change	Adjusted <i>P</i> value
<i>Trp63</i>	1.63	1.49E-03
<i>Jag2</i>	1.34	2.47E-02
<i>Itgb4</i>	1.44	9.8E-03
<i>Krt15</i>	4.11	5.5E-05
<i>Krt4</i>	2.33	1.0E-05
<i>Krt17</i>	2.25	1.0E-02

Trp63+ cells in *Shh^{cre}:Ezh2^{fllox/fllox}* mutants express additional markers of the basal cell lineage and are of lung origin

To assess whether the Trp63+ cells in *Shh^{cre}:Ezh2^{fllox/fllox}* mutant lungs expressed other markers of the basal cell lineage, we performed IHC for Krt5, Krt14 and Podoplanin (Pdpn). *Krt5* and *Krt14* are known transcriptional targets of Trp63 (Romano et al.,

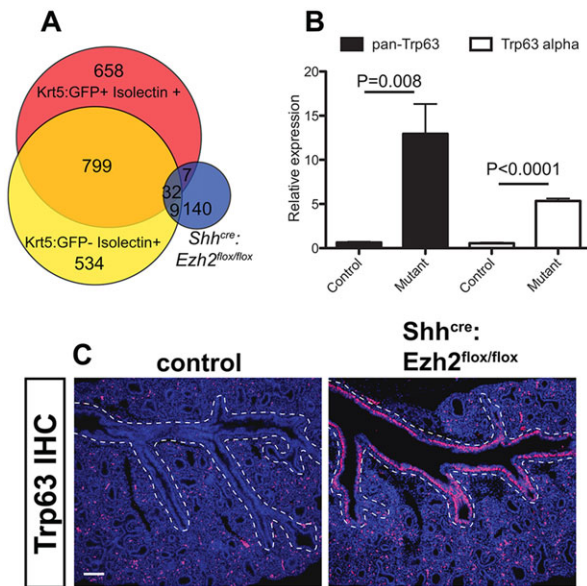


Fig. 3. Transcriptome analysis indicates ectopic basal cell formation in *Shh^{cre}:Ezh2^{flox/flox}* mutant lungs. (A) Comparison between two previously published microarray analyses of mouse tracheal basal cells shows significant overlap between *Shh^{cre}:Ezh2^{flox/flox}* mutant lungs and tracheal basal cells. (B) Pan-Trp63 and Trp63 alpha isoforms are both upregulated, as determined by qPCR in *Shh^{cre}:Ezh2^{flox/flox}* mutant lungs at E14.5. (C) IHC for Trp63 in control and *Shh^{cre}:Ezh2^{flox/flox}* mutant lungs at E14.5. Note Trp63+ cells lining the entire airways of *Shh^{cre}:Ezh2^{flox/flox}* mutant lungs (dashed lines); non-specific signal from blood cells can be seen outside the dotted lines. Scale bar: 100 μm.

2007, 2009). Krt5, Krt14 and Pdpn are not expressed in airway epithelium of control lungs at E16.5 (Fig. 4A). By contrast, Krt5 expression is observed at E16.5 throughout the developing airway epithelium of *Shh^{cre}:Ezh2^{flox/flox}* mutant lungs (Fig. 4A). This corresponds to the expansion of Trp63 in *Shh^{cre}:Ezh2^{flox/flox}* mutant lungs (Fig. 4A). Krt14 is also observed in *Shh^{cre}:Ezh2^{flox/flox}* mutant lungs at E16.5 but is restricted to the basal cell layer along with Pdpn (Fig. 4A, inset). Pax9, which is normally expressed in Trp63+ cells of the esophagus (Peters et al., 1998), is also highly expressed in *Shh^{cre}:Ezh2^{flox/flox}* mutant lung airways at E16.5 (Fig. 4A). The increase or ectopic expression of Krt5, Krt14, Pdpn and Pax9 was confirmed by qPCR (Fig. 4B).

Because physical association of a locus with *Ezh2* does not necessarily correlate with active repression *in vivo* (Davidovich et al., 2013; Cifuentes-Rojas et al., 2014), we performed ChIP against the histone mark H3K27me3, which is associated with *Ezh2*/PRC2 repression, on the promoters of several of the upregulated genes. The promoters for the basal cell genes *dNp63*, *Krt5* and *Krt14* have little enrichment for the H3K27me3 histone mark relative to a gene desert region or the actively transcribed gene *Gapdh* (Fig. 4C). However, the promoter of *Pax9*, which is highly expressed in the airways of *Shh^{cre}:Ezh2^{flox/flox}* mutant lungs and is known to be expressed in Trp63+ esophageal basal cells (Peters et al., 1998), shows a high level of H3K27me3 histone marks (Fig. 4C). Of note, other Pax family members have previously been shown to be repressed by *Ezh2* (Woodhouse et al., 2013).

To test whether the increased expression of Pax9 could lead to initiation of some or all aspects of the basal cell program during lung development, we overexpressed Pax9 in the developing lung endoderm using the well-characterized human *SFTPC* promoter and observed Trp63-expressing cells in both large and small airways of transgenic lungs at E17.5 (Fig. 4D,E). Moreover, *Scgblal*

expression was also decreased upon Pax9 overexpression, consistent with the data from *Shh^{cre}:Ezh2^{flox/flox}* mutant lungs (Fig. 4E). These data suggest that Pax9 de-repression is partially responsible for the increase in Trp63 expression in *Shh^{cre}:Ezh2^{flox/flox}* mutant lungs. However, we could not detect expression of other basal cell markers, including Pdpn, Krt5 and Krt14, in the *SFTPC*-Pax9 transgenic lungs (data not shown), suggesting that Pax9 is not the sole driver of this phenotype.

To assess whether the Trp63+ basal cells in the airways of *Shh^{cre}:Ezh2^{flox/flox}* mutant lungs expressed Nkx2-1 and thus exhibit lung endoderm identity despite expressing Pax9, co-IHC was performed for Trp63 and Nkx2-1 at E18.5. These data show that the Trp63+ basal cells in *Shh^{cre}:Ezh2^{flox/flox}* mutant lungs co-express Nkx2-1 similar to basal cells that normally form in the adult lung trachea and main stem bronchi (Fig. 5A). Moreover, these data show that the mutant airway epithelium is no longer organized into a single monolayer of cells. Whereas the Trp63+ basal cells are located in a basal position, there appear to be multiple layers of Nkx2-1+ epithelial cells overlaying these (Fig. 5A). Thus, the ectopic appearance of Trp63+ basal cells in *Shh^{cre}:Ezh2^{flox/flox}* mutant lungs leads to formation of a multilayered and disorganized epithelial layer lining the bronchiolar airways.

Ectopic Trp63+ basal cells develop early upon loss of *Ezh2* expression in the lung

To determine when Trp63+ basal cells start to develop in the proximal airways of the *Shh^{cre}:Ezh2^{flox/flox}* mutants, we performed co-IHC for Sox2 and Trp63. Whereas only rarely observed in E12.5 control lungs, numerous Trp63+/Sox2+ cells could be observed in *Shh^{cre}:Ezh2^{flox/flox}* mutant lungs even at this early time point (Fig. 5B). Moreover, these Trp63+/Sox2+ cells became more numerous as development progressed through E18.5. Of note, all Trp63+ cells expressed Sox2, thus suggesting that they arose from a primitive Sox2+ lung endoderm progenitor early in airway development.

Next, we assessed the expression time course of the basal cell markers Krt5, Krt14 and Pdpn. Whereas Trp63+ cells appeared by E12.5, Krt5 expression was not observed until E14.5, when Krt5 became detectable in some Trp63+ cells in the bronchioles of *Shh^{cre}:Ezh2^{flox/flox}* mutant lungs (Fig. 5C). By E18.5, Krt5 expression was observed throughout the developing airway epithelium, including dome-shaped cells that were not in the basal position (Fig. 5C). Krt14 and Pdpn expression lagged behind Krt5, and these markers were not present in Trp63+ cells at E14.5 (Fig. 5D,E). By E18.5, the expression of Krt14 and Pdpn was expanded to a majority of Trp63+ basal cells in the bronchioles of *Shh^{cre}:Ezh2^{flox/flox}* mutant lungs (Fig. 5D,E). Thus, basal cells form earlier and at much higher numbers upon loss of *Ezh2* in the developing lung epithelium.

Ectopic basal cell development does not result in perturbed neuroendocrine or goblet cell development

As the ectopic appearance of basal cells in the developing lung airways of *Shh^{cre}:Ezh2^{flox/flox}* mutants could perturb the differentiation of other airway epithelial cell lineages, we assessed whether there were any effects on neuroendocrine and goblet cell lineages. Both IHC (Fig. 6A) and qPCR (Fig. 6B) for the neuroendocrine marker *Pgp9.5* shows that ectopic development of basal cells in *Shh^{cre}:Ezh2^{flox/flox}* mutant lungs does not affect the overall development of neuroendocrine cells. Moreover, IHC for the goblet cell marker *Muc5ac* did not reveal an increase in the goblet cell lineage in *Shh^{cre}:Ezh2^{flox/flox}* mutant lungs (Fig. 6C). These data

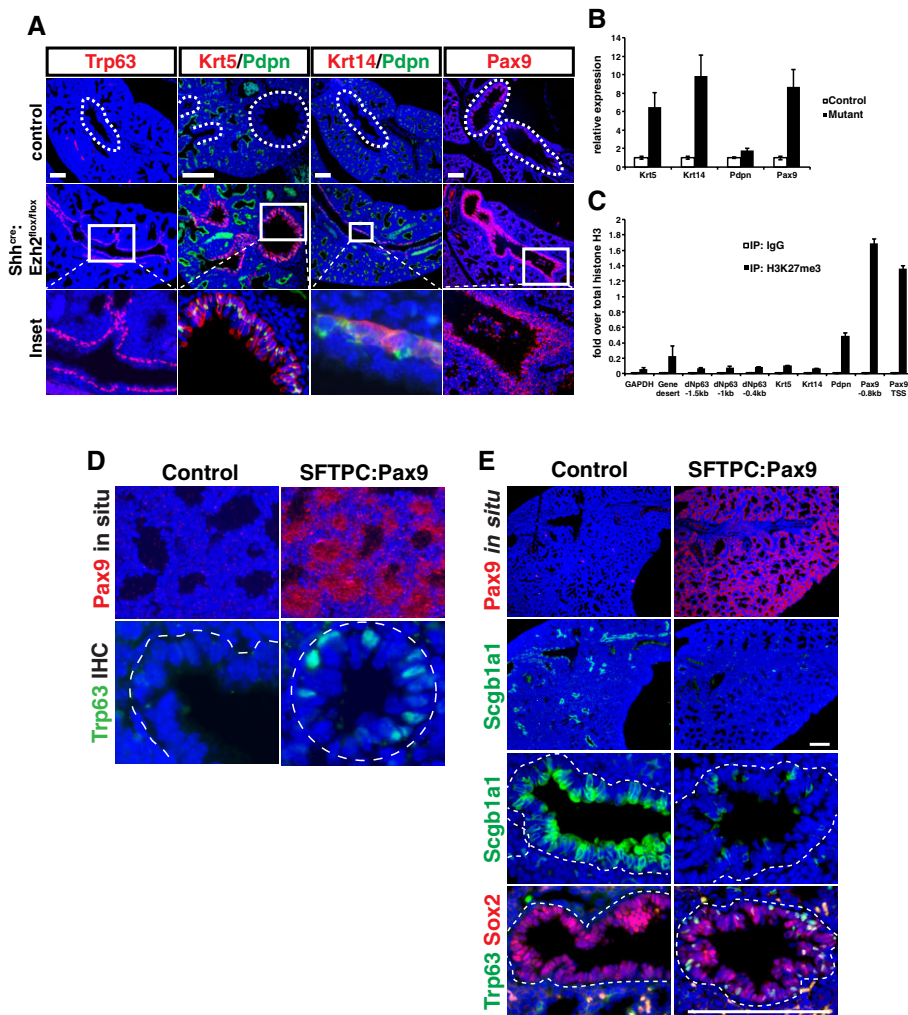


Fig. 4. Expression of basal cell markers in *Shh^{cre}:Ezh2^{lox/lox}* mutant lungs. (A) IHC for Trp63, Krt5, Krt14 and Pdpn, and *in situ* hybridization (ISH) for Pax9 expression patterns at E16.5 in control and *Shh^{cre}:Ezh2^{lox/lox}* mutant lungs. Dotted lines outline the airways of each lung, and bottom row shows higher magnification of boxed regions of basal cells expressing the respective markers. Note expression of Krt5 throughout the airway epithelium of *Shh^{cre}:Ezh2^{lox/lox}* mutant lungs, including dome-shaped cells, whereas Krt14 and Pdpn are restricted to basal cells in these mutants. (B) qPCR revealing increased expression of Krt5, Krt14, Pdpn and Pax9 in *Shh^{cre}:Ezh2^{lox/lox}* mutant lungs at E16.5. (C) ChIP-qPCR for H3K27me3 occupancy of basal cell gene promoters in wild-type lungs at E12.5. Note that the Pax9 but not the dNp63 promoter is enriched for H3K27me3 relative to the *Gapdh* promoter. (D) Ectopic expression of the Pax9 cDNA and ectopic appearance of Trp63+ cells in the airways in *SFTPC-Pax9* transgenic lungs at E17.5. (E) Decreased *Scgb1a1* expression correlates with ectopic expression of Pax9 and appearance of Trp63+ cells in *SFTPC-Pax9* transgenic lungs at E17.5. Dashed lines (D,E) outline the airway epithelium. Scale bars: 100 μ m.

indicate that differentiation of other proximal epithelial lineages, including neuroendocrine and goblet cells, was not affected by loss of *Ezh2* or the ectopic development of basal cells.

Cell proliferation in *Shh^{cre}:Ezh2^{lox/lox}* mutant lungs

As the ectopic appearance of Trp63+ basal cells in *Shh^{cre}:Ezh2^{lox/lox}* mutant lungs could be due to an increase in cell proliferation of a small number of these cells early in development, we assessed both the overall cell proliferation changes as well as the specific changes in Trp63+ and Sox2+ cells in *Shh^{cre}:Ezh2^{lox/lox}* mutant lungs. Both at E12.5 and at E14.5, there was no significant overall change in cell proliferation in *Shh^{cre}:Ezh2^{lox/lox}* mutant lungs as measured by phosphorylated histone 3 (PH3) (Fig. 6D). However, by E18.5, there was a significant decrease in epithelial cell proliferation in *Shh^{cre}:Ezh2^{lox/lox}* mutant lungs (Fig. 6E). We used 5-bromo-2'-deoxyuridine (BrdU) labeling to measure the specific proliferation rates in Sox2+ proximal airway epithelial cells at E12.5 and found no significant changes in their proliferation in *Shh^{cre}:Ezh2^{lox/lox}* mutant lungs (Fig. 6F). To determine whether the Trp63+ population expanded between E12.5 and E14.5 due to a higher proliferation rate than the rest of the Sox2+ epithelium, we compared the proliferation rate of the ectopic Trp63+ cells with the rest of the Sox2+ epithelium, and found that Trp63+ cells do not have a proliferative advantage (Fig. 6F). Thus, it is unlikely that an increase in cell proliferation in a small number of Trp63+ cells early

in development could account for the dramatic increase in these cells in *Shh^{cre}:Ezh2^{lox/lox}* mutant lungs.

Trp63–/Krt5+ cells formed in *Shh^{cre}:Ezh2^{lox/lox}* mutant lungs resemble secretory cells and might represent an intermediate between the basal and secretory lineages

Closer examination of the Krt5+ population of cells in the E18.5 lung shows that, in addition to the basal cells expressing Krt5, there is also a large population of dome-shaped cells that express Krt5 (Fig. 7A). Whereas some of these cells express Trp63, there is a population of Trp63–/Krt5+ dome-shaped cells which contain nuclei on the luminal side of the airway (Fig. 7A, asterisks). This is in contrast to Pdpn expression, which is preferentially located to just basal cells in the airways of *Shh^{cre}:Ezh2^{lox/lox}* mutant lungs at E18.5 (Fig. 7B). This suggests that the dome-shaped Krt5+ cells are distinct from the basal Krt5+/Trp63+/Pdpn+ cells. The nuclei that protrude into the lumen could be due to interkinetic nuclear migration during cell division. However, PH3 or BrdU IHC did not indicate any active cell proliferation in these dome-shaped Krt5+ cells at E18.5 (Fig. 7C,D). Moreover, immunostaining for markers of the secretory lineage, including SSEA1 and *Scgb1a1*, shows that the Trp63–/Krt5+ dome-shaped cells do not express these genes and are not mature secretory cells (Fig. 7E). These dome-shaped Krt5+ cells also do not express the multiciliated epithelial marker TubbIV (Fig. 7E).

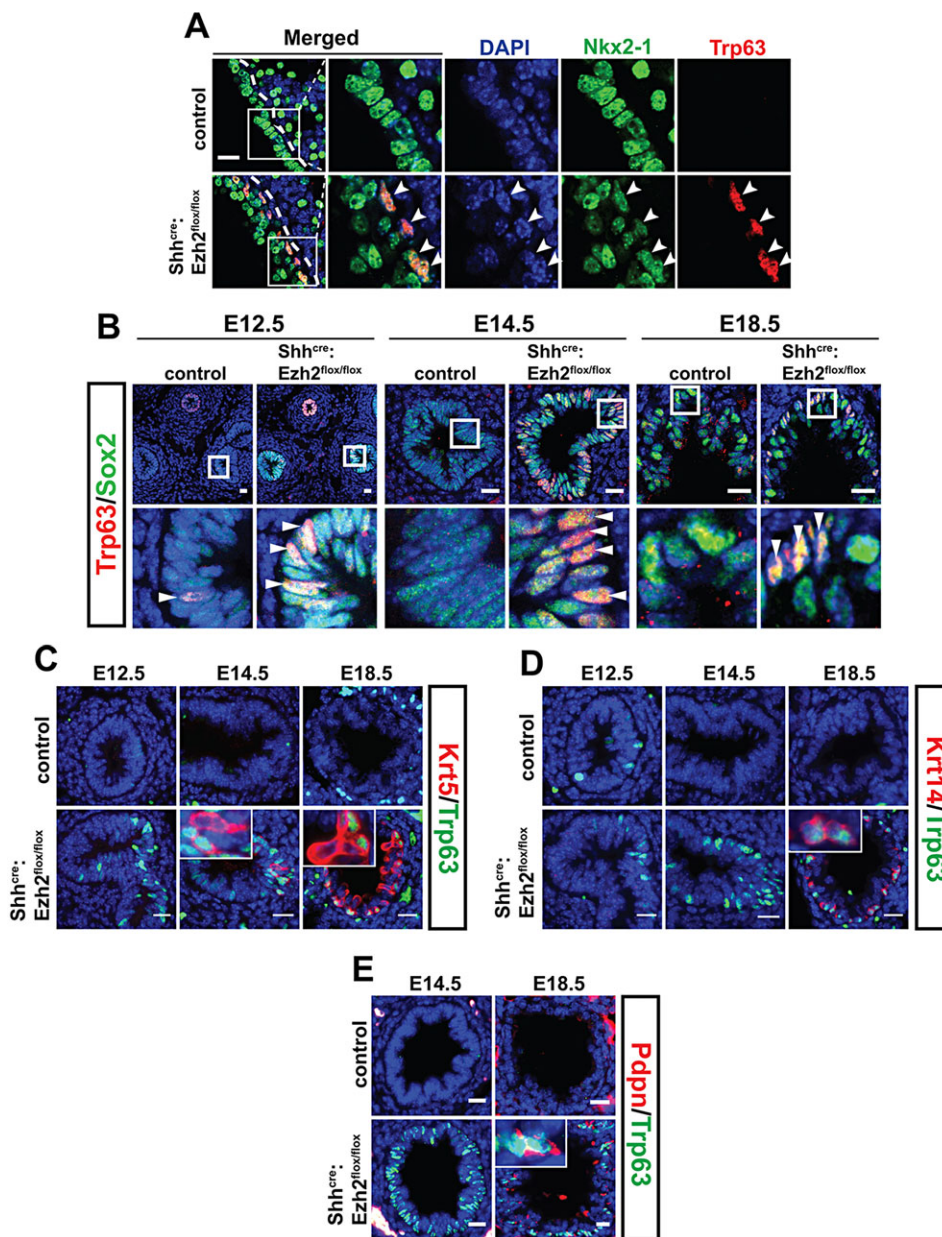


Fig. 5. Basal cells develop early in *Shh^{cre}; Ezh2^{flox/flox}* mutant lungs and express Nkx2-1. (A) Co-expression of Trp63 and Nkx2-1 in basal cells of *Shh^{cre}; Ezh2^{flox/flox}* mutant lungs at E18.5. Thick dashed lines demarcate airway epithelium. Boxed regions and thin dashed lines indicate regions magnified on the right. (B) Sox2 and Trp63 co-IHC shows that Trp63+ cells are observed at high frequency in *Shh^{cre}; Ezh2^{flox/flox}* mutant lungs as early as E12.5. These cells increase in frequency at both E14.5 and E18.5. Note that all Trp63+ cells express Sox2. Arrowheads indicate Trp63+ cells. Boxed regions are magnified beneath. (C) Time course of Krt5 expression showing that it lags Trp63 expression and is not observed until E14.5 in sporadic Trp63+ cells. By E18.5, all Trp63+ cells are Krt5+ and there are additional Krt5-expressing dome-shaped luminal cells. Insets show higher magnification of Krt5+ cells with and without Trp63 co-expression. (D) Time course of Krt14 expression showing that it lags behind Trp63 and Krt5 expression, but is expressed extensively at E18.5 in most Trp63+ basal cells. Insets show higher magnification of Krt14+ cells. Note that Krt14+ cells express Trp63. (E) At E14.5, Pdpn expression is not observed in Trp63+ cells in *Shh^{cre}; Ezh2^{flox/flox}* mutant lungs. However, by E18.5 Pdpn expression is observed in basal cells in *Shh^{cre}; Ezh2^{flox/flox}* mutant lungs but is not observed at significant levels in control airway epithelium. Insets show higher magnification of Pdpn+ cells. Note that Pdpn+ cells express Trp63. Scale bars: 20 μ m.

As previous studies have demonstrated an important role for Notch signaling in development of the secretory cell lineage (Tsao et al., 2009), we examined expression of the Notch1 intracellular domain (NICD) to assess activity of this pathway in *Shh^{cre}; Ezh2^{flox/flox}* mutant lungs. In the large bronchi of control animals, we observed a co-localization of NICD with Trp63 expression but there was no expression of either protein in the more distal bronchioles (supplementary material Fig. S3A). However, we observed co-localization of NICD and Trp63 in the distal bronchioles of *Shh^{cre}; Ezh2^{flox/flox}* mutant lungs at E14.5 (supplementary material Fig. S3A). This suggests that these basal cells are initiating a differentiation program into secretory cells that they are unable to complete, perhaps due to their inability to fully silence the basal cell program. We also tested whether Ezh2 was required for club cell homeostasis or regeneration after injury by generating *Scgb1a1^{cre}; Ezh2^{flox/flox}* mice. The *Scgb1a1^{cre}* line efficiently deletes genes beginning at around birth in the lung airway epithelium (Li et al., 2012). *Scgb1a1^{cre}; Ezh2^{flox/flox}* mice appeared normal and healthy and did

not exhibit any obvious defects in Scgb1a1 club cell homeostasis (supplementary material Fig. S3B). Moreover, naphthalene-induced injury to the secretory cells in *Scgb1a1^{cre}; Ezh2^{flox/flox}* mice did not result in a significant difference in the ability of the secretory cells to regenerate in comparison to control animals (supplementary material Fig. S3C).

These data indicate that, whereas Ezh2 restrains the basal cell lineage, it is also required for differentiation into the secretory cell lineage during development, and the Trp63–/Krt5+ cells might represent an intermediate between the basal and secretory cell fates (Fig. 7F). However, this regulation appears to be restricted to the developing lung endoderm, as postnatal loss of Ezh2 does not affect homeostasis or regeneration of the airway epithelium.

DISCUSSION

The epigenetic factors that help to pattern the lung epithelium are poorly understood. In this report, we show that Ezh2 is required to restrict the basal cell lineage, an important stem cell population

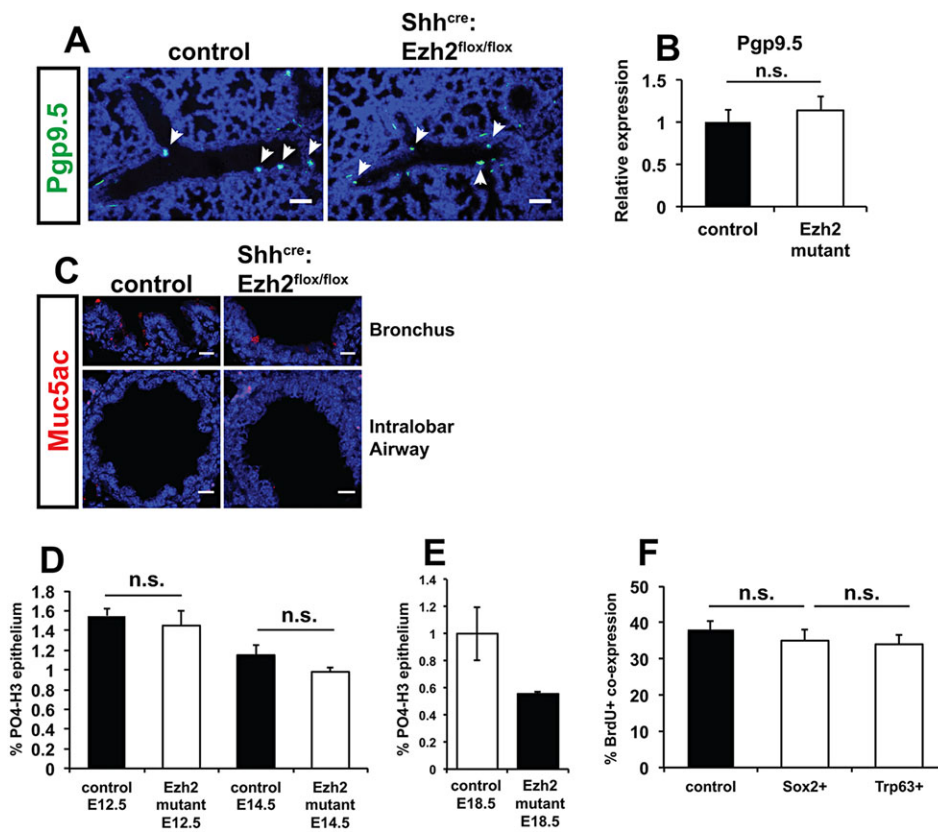


Fig. 6. Expression of neuroendocrine and goblet cell markers and assessment of cell proliferation in ectopic basal cells in *Shh^{cre}; Ezh2^{flox/flox}* mutant lungs. (A) Expression of Pgp9.5 by IHC is unaltered in *Shh^{cre}; Ezh2^{flox/flox}* mutant lungs at E18.5. Arrowheads indicate Pgp9.5+ neuroendocrine cells in neuroepithelial bodies. (B) qPCR of Pgp9.5 in control and *Shh^{cre}; Ezh2^{flox/flox}* mutant lungs at E18.5. (C) IHC of Muc5ac in control and *Shh^{cre}; Ezh2^{flox/flox}* mutant lungs at E18.5. (D) Cell proliferation in both control and *Shh^{cre}; Ezh2^{flox/flox}* mutant lungs at E12.5 and E14.5 as assessed by PH3 IHC. (E) Cell proliferation in both control and *Shh^{cre}; Ezh2^{flox/flox}* mutant lungs at E18.5 as assessed by PH3 IHC. (F) Cell proliferation assessed specifically in Sox2+ proximal epithelial cells in control and in *Shh^{cre}; Ezh2^{flox/flox}* mutant lungs at E12.5. n.s., not significant. Scale bars: 100 μ m in A, 20 μ m in C.

in the adult airways. Normally, in the mouse respiratory system, Trp63+ basal cells do not appear until right before birth and are only found lining the trachea and main stem bronchi. Loss of *Ezh2* early in mouse lung endoderm development results in the ectopic formation of Trp63+ basal cells as early as E12.5 in the lung airways. Moreover, the Trp63+ basal cells extend more distally into the developing lungs, including all the way to the bronchioalveolar junction. This ectopic formation of basal cells is coincident with a defect in secretory cell differentiation, including the formation of Trp63–/Krt5+ luminal cells that resemble secretory cells in shape but lack markers of differentiated secretory cells. These data indicate that *Ezh2* regulates both the temporal and spatial patterning of basal cells within the developing lung, and that it is also crucial for secretory cell differentiation.

Basal cells are the repopulating stem cell population in the postnatal trachea, differentiating into and replenishing the secretory club cell lineage (Rawlins et al., 2009; Rock et al., 2009). This stem cell function has not been demonstrated in the developing lungs, as tracheal basal cells usually develop shortly prior to birth and after most prenatal lung development (Rock and Hogan, 2011). The Trp63–/Krt5+ cells with club cell morphology suggests that the *Shh^{cre}; Ezh2^{flox/flox}* ectopic basal cells are attempting to differentiate into club cells but are unable to fully silence the basal cell program even after a reduction in Trp63 expression. Interestingly, Scgb1a1+ club cells are known to generate multiciliated cells in the adult lung (Rawlins et al., 2009). Our data, showing that the TubbIV+ multiciliated lineage is not affected upon loss of *Ezh2*, whereas the Scgb1a1+ club cell lineage is, suggests that these two lineages arise independently from a common Sox2+ progenitor during development.

Whereas the mouse remains an important model of lung and trachea development, there are distinct differences between mouse

and human airways. One of these differences is in the distribution of Trp63+ basal cells. As we have shown in our current report, Trp63+ basal cells are not found in significant numbers prior to E18.5 in the mouse lung and even then are found only sporadically and only in the trachea and main stem bronchi. By contrast, Trp63+ basal cells are found lining the entire airway in the human lung. Our studies show that loss of *Ezh2* in mouse lung development leads to the premature and ectopic formation of Trp63+ basal cells that underlie almost the entire airway all the way to the bronchioalveolar junction. Interestingly, Trp63+ cells were not found in the alveolar region, suggesting that *Ezh2* restricts the basal cell lineage only in the Sox2+ endoderm progenitor population. Together, these data indicate that *Ezh2* regulates the temporal and spatial patterning of the basal cell lineage in the mouse lung. A recent report showed that Trp63+ basal cells were enriched on the side of the trachea that developed cartilaginous rings during development (Hines et al., 2013). Loss of cartilage in the lung mesenchyme leads to a loss of Trp63+ basal cells, suggesting an important mesenchymal-epithelial cross-talk that regulates basal cell development. Our data indicate that *Ezh2*, and PRC2 in general, acts as a crucial integrator of the basal cell differentiation program in a cell-intrinsic manner.

The finding of Krt5+ luminal cells that do not express other markers of the basal lineage (i.e. Trp63, Pdpn) and do not express markers of the mature secretory cell lineage (i.e. SSEA1, Scgb1a1) suggests that *Ezh2* also regulates the differentiation of secretory cells during lung development. At least two possible scenarios could underlie such regulation: first, *Ezh2* might restrict the basal cell lineage and thereby shunt the differentiation of Sox2+ proximal endoderm progenitors towards basal cells and away from secretory cells. Second, the ectopic development of basal cells might offer a different mode of generating secretory cells in *Shh^{cre}; Ezh2^{flox/flox}* mutant lungs, but these cells cannot fully differentiate and appear

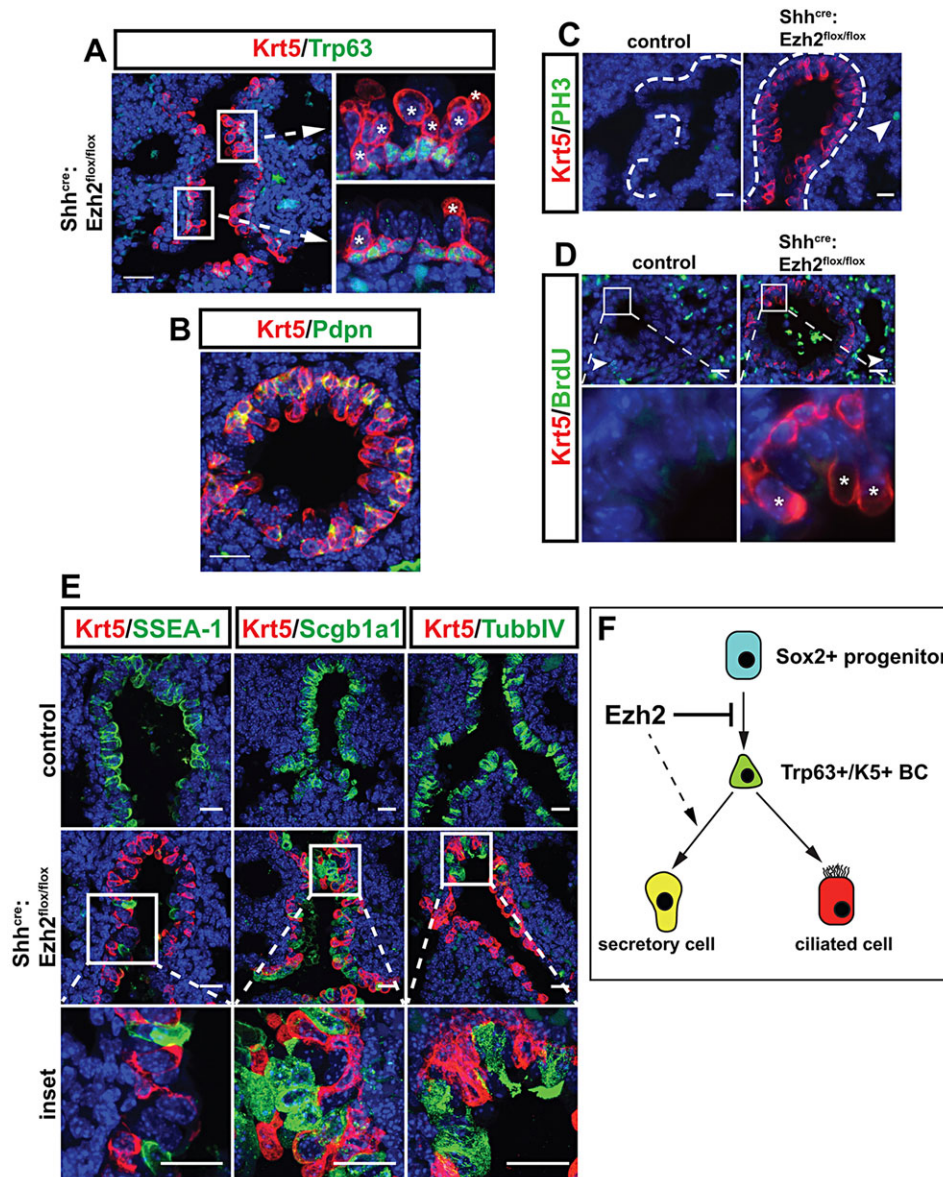


Fig. 7. Trp63⁺/Krt5⁺ cells line the airways of *Shh^{cre}:Ezh2^{flox/flox}* mutant lungs and are distinct from secretory and ciliated airway epithelial cells. (A) Expression of Krt5 is observed in both Trp63⁺ basal cells as well as Trp63-negative dome-shaped luminal cells (asterisks) lining *Shh^{cre}:Ezh2^{flox/flox}* mutant lungs at E18.5. Subpanels on the right show higher magnification of boxed regions on the left. (B) Basal cell marker Pdpn is not expressed in these Krt5 luminal cells in *Shh^{cre}:Ezh2^{flox/flox}* mutant lungs. (C, D) Krt5⁺ cells in the airway lumen are negative for the proliferation markers PH3 (C) and BrdU (D) at E18.5, suggesting that Krt5 cells are not temporarily protruding into the airway lumen during cell division. Arrowheads indicate nuclei positive for PH3 (C) and BrdU (D). Asterisks in D indicate the nuclei of Krt5⁺ luminal cells, which are negative for BrdU. Dashed lines in C demarcate the airway epithelium. Subpanels at the bottom of D show higher magnification of boxed regions in subpanels above. (E) Krt5 dome-shaped luminal cells do not express the secretory lineage markers SSEA1 and Scgb1a1 or the ciliated epithelium marker TubbIV. Subpanels at the bottom show higher magnification of boxed regions in subpanels above. Scale bars: 20 μ m. (F) Model of how Ezh2 restricts the Trp63⁺ basal cell lineage during mouse Sox2⁺ proximal endoderm progenitor development. Ezh2 is subsequently required for differentiation of airway endoderm progenitors into the secretory cell lineage. Whether this is due to a direct block to differentiation of Sox2⁺ secretory cell progenitors or whether this is due to these progenitors developing a Trp63⁺ basal cell fate and a subsequent block of these cells to differentiate into secretory cells remains unclear.

‘stuck’ in between the basal and secretory cell lineage. There is extensive evidence that basal cells both self-renew as well as differentiate into secretory and ciliated cells in the adult lung. Moreover, there is now data available showing that secretory cells and basal cells can interconvert between each phenotypic state. The Trp63⁺/Krt5⁺ population might represent either or both scenarios and does suggest a crucial role for Ezh2/PRC2 in regulating such an interconversion.

MATERIALS AND METHODS

Animals

CD-1 mice (Charles River) were used for characterization of Ezh2 expression by RNA-seq and Ezh2 IHC. *Shh^{cre}*, *Scgb1a1^{cre}* and *Ezh2^{flox/flox}* mice and their genotyping have been previously described (Su et al., 2003; Harfe et al., 2004; Li et al., 2012). BrdU was administered intraperitoneally (30 mg/kg body weight) 45 min prior to dissection. Naphthalene was administered intraperitoneally as previously described (Li et al., 2012), to male mice 8–12 weeks old at a dose of 250 mg/kg body weight. Regeneration was analyzed at 15 days post injury.

To generate *SFTPC-Pax9* mice, the full mouse Pax9 coding region was cloned downstream of the human 3.7 kb *SFTPC* promoter and upstream of a

SV40 polyadenylation sequence as previously described (Tian et al., 2011). The transgenic cassette was excised from the resulting plasmid, purified and injected into FVB/N fertilized oocytes. Transgenic embryos were collected at E17.5 and genotyped using the PCR primers listed in supplementary material Table S2. Two independent F0 genotype-positive animals were analyzed for these studies. All animal procedures were performed in accordance with the Institute for Animal Care and Use Committee at the University of Pennsylvania.

Microarray experiments

E14.5 lungs were isolated from four *Shh^{cre}* control and four *Shh^{cre}:Ezh2^{flox/flox}* mutant lungs. Lungs were collected into RNAlater (Life Technologies) and stored overnight at 4°C, then snap-frozen in liquid nitrogen and stored at –80°C until use. RNA was isolated using the RNeasy Mini Kit (Qiagen) according to the manufacturer’s protocol. Biotinylated cRNA probe libraries were generated from these RNA samples and used with Affymetrix Mouse Gene 2.0ST arrays. Microarray data were analyzed using the Oligo package available at the Bioconductor website (<http://www.bioconductor.org>). The raw data were background-corrected by the robust multichip average (RMA) method and then normalized by an invariant set method. Differential gene expression between the control and mutant mice was analyzed by the Limma package available at the Bioconductor website. *P* values obtained from the

multiple comparison tests were corrected by false discovery rates. See supplementary material Table S1 for the full list of genes that were significantly altered. To compare this microarray with publicly available microarray data from Rock et al. (2009), data were normalized by variance stabilization transformation and analyzed as described. The GEO accession number for the microarray data is GSE60660.

Quantitative RT-PCR

Total RNA was isolated using TRIzol (Life Technologies). cDNA was synthesized using Superscript III reverse transcriptase (Life Technologies) with Oligo(dT) primers. Quantitative RT-PCR was performed using a 7900HT Fast Real-Time PCR System machine and SDS2.3 software (Applied Biosystems). Gene expression levels were normalized to *Gapdh*. Statistical analysis was performed on GraphPad Prism software, using one-tailed Welch's *t*-test for unequal variances. Primers are listed in supplementary material Table S2.

ChIP-qPCR

Lungs were isolated at E12.5 from CD-1 mice and processed using the chromatin immunoprecipitation kit (Millipore) according to the manufacturer's instructions. Ten lungs were used per sample. Lungs were crosslinked for 15 min and sonicated to an average of 200 bp using a Diagenode Bioruptor. Immunoprecipitation was performed using the following antibodies: rabbit IgG, rabbit anti-histone 3 (pan) and rabbit anti-H3K27me3 (Millipore 12-370, 07-690, 07-449, respectively; 5 µg antibody or IgG per immunoprecipitation reaction). ChIP was analyzed by quantitative real-time PCR using the primers listed in supplementary material Table S2.

Histology

Tissues were fixed in fresh 2% or 4% paraformaldehyde, embedded in paraffin wax and sectioned at a thickness of 6–8 µm. Hematoxylin and Eosin (H&E) staining was performed using standard procedures. *In situ* hybridization and IHC were performed as described (Wang and Morrisey, 2010; Tian et al., 2011; Li et al., 2012; Wang et al., 2013). IHC used the following antibodies: anti-β-tubulin/IV/TubbIV (BioGenex, MU178-UC; 1:20); anti-BrdU, anti-mucin5AC, anti-Scgb3a2 (Abcam, ab6326, ab3649, ab8875, respectively; 1:100, 1:100, 1:50, respectively); anti-Pgp9.5 (AnaSpec, 53772; 1:200); anti-phospho-histone 3, anti-Ezh2, anti-cleaved notch 1 intracellular domain (Cell Signaling Technology, 9706L, 5246, 4147, respectively; 1:200, 1:100, 1:50, respectively); anti-keratin 5, anti-keratin 14 (Covance, PRB-160P, PRB-155P, respectively; 1:1500, 1:1000, respectively); anti-T1a/Pdpn (Hybridoma Bank Clone 8.1.1; 1:50); anti-SSEA-1, anti-prosulfactant protein C (EMD Millipore, MAB4301, AB3786, respectively; 1:100, 1:500, respectively); anti-CC-10/Scgb1a1, anti-p63, anti-TTF1/Nkx2.1, anti-Sox9 (Santa Cruz Biotechnology, sc-9772, sc-8431, sc-25268, sc-8343, sc-13040, sc-20095, respectively; 1:20, 1:10, 1:50, 1:200, 1:50, 1:100, respectively); anti-Sox2 (Seven Hills Bioreagents, WRAB-SOX2; 1:500). Terminal deoxynucleotidyl transferase dUTP nick end labeling (TUNEL) (Roche) was performed according to the manufacturer's directions. Slides were mounted with Vectashield mounting medium containing DAPI (Vector Laboratories). PH3+ nuclei were counted by hand and normalized to the area of the lung section. Statistical analysis was performed on GraphPad Prism software, using the one-tailed Welch's *t*-test for unequal variances. *P* values greater than 0.05 were considered to be not significant.

Acknowledgements

The authors gratefully acknowledge Ying Tian for helpful discussion, the Penn CVI Histology Core for histology services and Andrea Stout for help with confocal microscopy.

Competing interests

The authors declare no competing financial interests.

Author contributions

M.E.S. designed these studies and performed experiments; S.L. designed and generated transgenic animals and *in situ* probes; M.P.M. and K.R. performed

bioinformatics analysis; and M.M.L. performed histological experiments. R.S.K. provided technical assistance; M.E.S., K.M.S. and E.E.M. analyzed data; and M.E.S. and E.E.M. wrote the manuscript.

Funding

These studies were supported by funding from the National Institutes of Health [HL071589, HL087825, HL100405 and HL110942]. Deposited in PMC for release after 12 months.

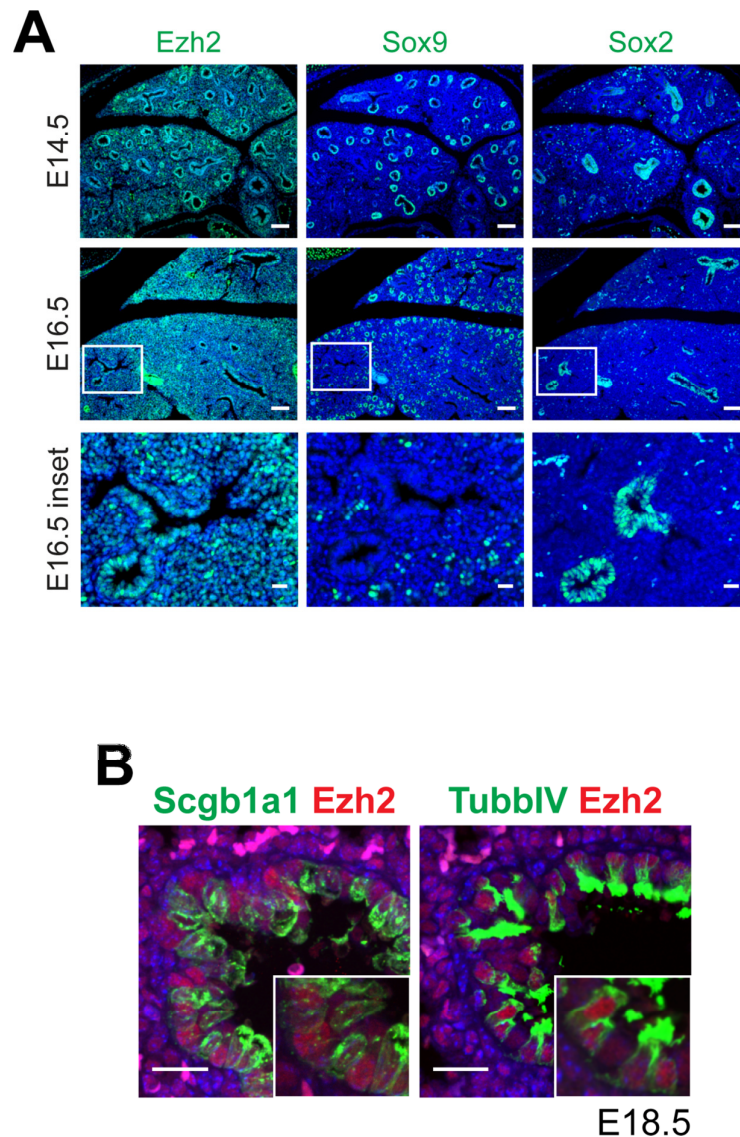
Supplementary material

Supplementary material available online at <http://dev.biologists.org/lookup/suppl/doi:10.1242/dev.116947/-/DC1>

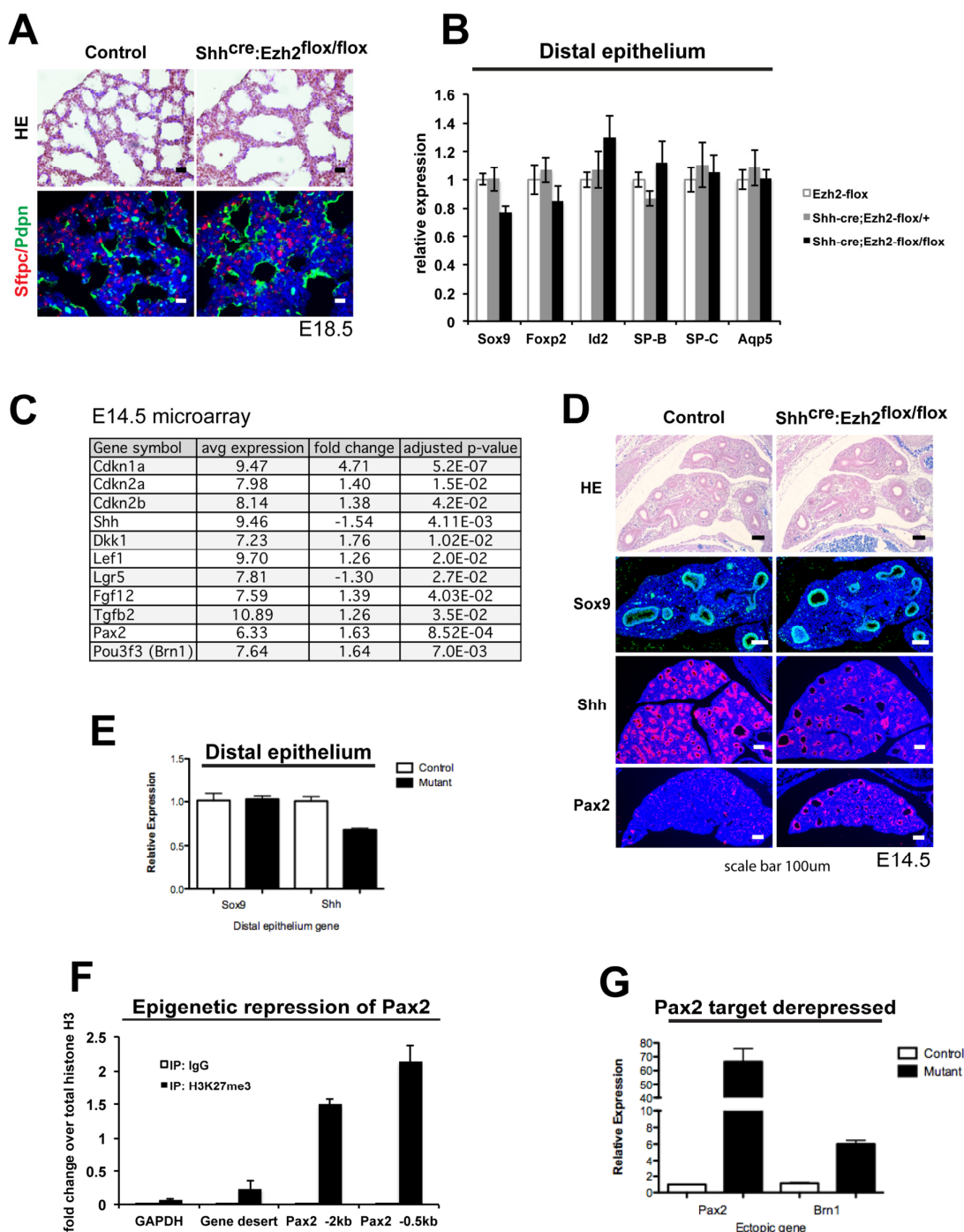
References

- Blobel, G. A., Moll, R., Franke, W. W. and Vogt-Moykopf, I. (1984). Cytokeratins in normal lung and lung carcinomas. I. Adenocarcinomas, squamous cell carcinomas and cultured cell lines. *Virchows Arch.* **45**, 407–429.
- Cifuentes-Rojas, C., Hernandez, A. J., Sarma, K. and Lee, J. T. (2014). Regulatory interactions between RNA and polycomb repressive complex 2. *Mol. Cell* **55**, 171–185.
- Davidovich, C., Zheng, L., Goodrich, K. J. and Cech, T. R. (2013). Promiscuous RNA binding by Polycomb repressive complex 2. *Nat. Struct. Mol. Biol.* **20**, 1250–1257.
- Harfe, B. D., Scherz, P. J., Nissim, S., Tian, H., McMahon, A. P. and Tabin, C. J. (2004). Evidence for an expansion-based temporal Shh gradient in specifying vertebrate digit identities. *Cell* **118**, 517–528.
- Herriges, M. and Morrisey, E. E. (2014). Lung development: orchestrating the generation and regeneration of a complex organ. *Development* **141**, 502–513.
- Herriges, M. J., Swarr, D. T., Morley, M. P., Rath, K. S., Peng, T., Stewart, K. M. and Morrisey, E. E. (2014). Long noncoding RNAs are spatially correlated with transcription factors and regulate lung development. *Genes Dev.* **28**, 1363–1379.
- Hines, E. A., Jones, M.-K. N., Verheyden, J. M., Harvey, J. F. and Sun, X. (2013). Establishment of smooth muscle and cartilage juxtaposition in the developing mouse upper airways. *Proc. Natl. Acad. Sci. USA* **110**, 19444–19449.
- Kimura, S., Hara, Y., Pineau, T., Fernandez-Salguero, P., Fox, C. H., Ward, J. M. and Gonzalez, F. J. (1996). The *Tebp* null mouse: thyroid-specific enhancer-binding protein is essential for the organogenesis of the thyroid, lung, ventral forebrain, and pituitary. *Genes Dev.* **10**, 60–69.
- Li, S., Wang, Y., Zhang, Y., Lu, M. M., DeMayo, F. J., Dekker, J. D., Tucker, P. W. and Morrisey, E. E. (2012). Foxp1/4 control epithelial cell fate during lung development and regeneration through regulation of anterior gradient 2. *Development* **139**, 2500–2509.
- Liu, C., Morrisey, E. E. and Whitsett, J. A. (2002). GATA-6 is required for maturation of the lung in late gestation. *Am. J. Physiol. Lung Cell Mol. Physiol.* **283**, L468–L475.
- Peters, H., Neubuser, A., Kratochwil, K. and Balling, R. (1998). Pax9-deficient mice lack pharyngeal pouch derivatives and teeth and exhibit craniofacial and limb abnormalities. *Genes Dev.* **12**, 2735–2747.
- Que, J., Okubo, T., Goldenring, J. R., Nam, K.-T., Kurotani, R., Morrisey, E. E., Taranova, O., Pevny, L. H. and Hogan, B. L. M. (2007). Multiple dose-dependent roles for Sox2 in the patterning and differentiation of anterior foregut endoderm. *Development* **134**, 2521–2531.
- Que, J., Luo, X., Schwartz, R. J. and Hogan, B. L. M. (2009). Multiple roles for Sox2 in the developing and adult mouse trachea. *Development* **136**, 1899–1907.
- Rawlins, E. L., Okubo, T., Xue, Y., Brass, D. M., Auten, R. L., Hasegawa, H., Wang, F. and Hogan, B. L. M. (2009). The role of Scgb1a1+ Clara cells in the long-term maintenance and repair of lung airway, but not alveolar, epithelium. *Cell Stem Cell* **4**, 525–534.
- Rock, J. R. and Hogan, B. L. M. (2011). Epithelial progenitor cells in lung development, maintenance, repair, and disease. *Annu. Rev. Cell Dev. Biol.* **27**, 493–512.
- Rock, J. R., Onaitis, M. W., Rawlins, E. L., Lu, Y., Clark, C. P., Xue, Y., Randell, S. H. and Hogan, B. L. M. (2009). Basal cells as stem cells of the mouse trachea and human airway epithelium. *Proc. Natl. Acad. Sci. USA* **106**, 12771–12775.
- Rock, J. R., Randell, S. H. and Hogan, B. L. M. (2010). Airway basal stem cells: a perspective on their roles in epithelial homeostasis and remodeling. *Dis. Model. Mech.* **3**, 545–556.
- Rockich, B. E., Hrycaj, S. M., Shih, H. P., Nagy, M. S., Ferguson, M. A. H., Kopp, J. L., Sander, M., Wellik, D. M. and Spence, J. R. (2013). Sox9 plays multiple roles in the lung epithelium during branching morphogenesis. *Proc. Natl. Acad. Sci. USA* **110**, E4456–E4464.
- Romano, R.-A., Birkaya, B. and Sinha, S. (2007). A functional enhancer of keratin14 is a direct transcriptional target of deltaNp63. *J. Invest. Dermatol.* **127**, 1175–1186.
- Romano, R.-A., Ortt, K., Birkaya, B., Smalley, K. and Sinha, S. (2009). An active role of the DeltaN isoform of p63 in regulating basal keratin genes K5 and K14 and directing epidermal cell fate. *PLoS ONE* **4**, e5623.

- Signoretti, S., Waltregny, D., Dilks, J., Isaac, B., Lin, D., Garraway, L., Yang, A., Montironi, R., McKeon, F. and Loda, M. (2000). p63 is a prostate basal cell marker and is required for prostate development. *Am. J. Pathol.* **157**, 1769-1775.
- Su, I.-h., Basavaraj, A., Krutchinsky, A. N., Hobert, O., Ullrich, A., Chait, B. T. and Tarakhovsky, A. (2003). Ezh2 controls B cell development through histone H3 methylation and Igh rearrangement. *Nat. Immunol.* **4**, 124-131.
- Tata, P. R., Mou, H., Pardo-Saganta, A., Zhao, R., Prabhu, M., Law, B. M., Vinarsky, V., Cho, J. L., Breton, S., Sahay, A. et al. (2013). Dedifferentiation of committed epithelial cells into stem cells in vivo. *Nature* **503**, 218-223.
- Tian, Y., Zhang, Y., Hurd, L., Hannenhalli, S., Liu, F., Lu, M. M. and Morrisey, E. E. (2011). Regulation of lung endoderm progenitor cell behavior by miR302/367. *Development* **138**, 1235-1245.
- Tompkins, D. H., Besnard, V., Lange, A. W., Keiser, A. R., Wert, S. E., Bruno, M. D. and Whitsett, J. A. (2011). Sox2 activates cell proliferation and differentiation in the respiratory epithelium. *Am. J. Respir. Cell Mol. Biol.* **45**, 101-110.
- Tsao, P.-N., Vasconcelos, M., Izvolzky, K. I., Qian, J., Lu, J. and Cardoso, W. V. (2009). Notch signaling controls the balance of ciliated and secretory cell fates in developing airways. *Development* **136**, 2297-2307.
- Wang, Y. and Morrisey, E. (2010). Regulation of cardiomyocyte proliferation by Foxp1. *Cell Cycle* **9**, 4251-4252.
- Wang, Y., Tian, Y., Morley, M. P., Lu, M. M., Demayo, F. J., Olson, E. N. and Morrisey, E. E. (2013). Development and regeneration of Sox2+ endoderm progenitors are regulated by a Hdac1/2-Bmp4/Rb1 regulatory pathway. *Dev. Cell* **24**, 345-358.
- Woodhouse, S., Pugazhendhi, D., Brien, P. and Pell, J. M. (2013). Ezh2 maintains a key phase of muscle satellite cell expansion but does not regulate terminal differentiation. *J. Cell Sci.* **126**, 565-579.
- Xing, Y., Li, C., Li, A., Sridurongrit, S., Tiozzo, C., Bellusci, S., Borok, Z., Kaartinen, V. and Minoo, P. (2010). Signaling via Alk5 controls the ontogeny of lung Clara cells. *Development* **137**, 825-833.
- Yang, H., Lu, M. M., Zhang, L., Whitsett, J. A. and Morrisey, E. E. (2002). GATA6 regulates differentiation of distal lung epithelium. *Development* **129**, 2233-2246.

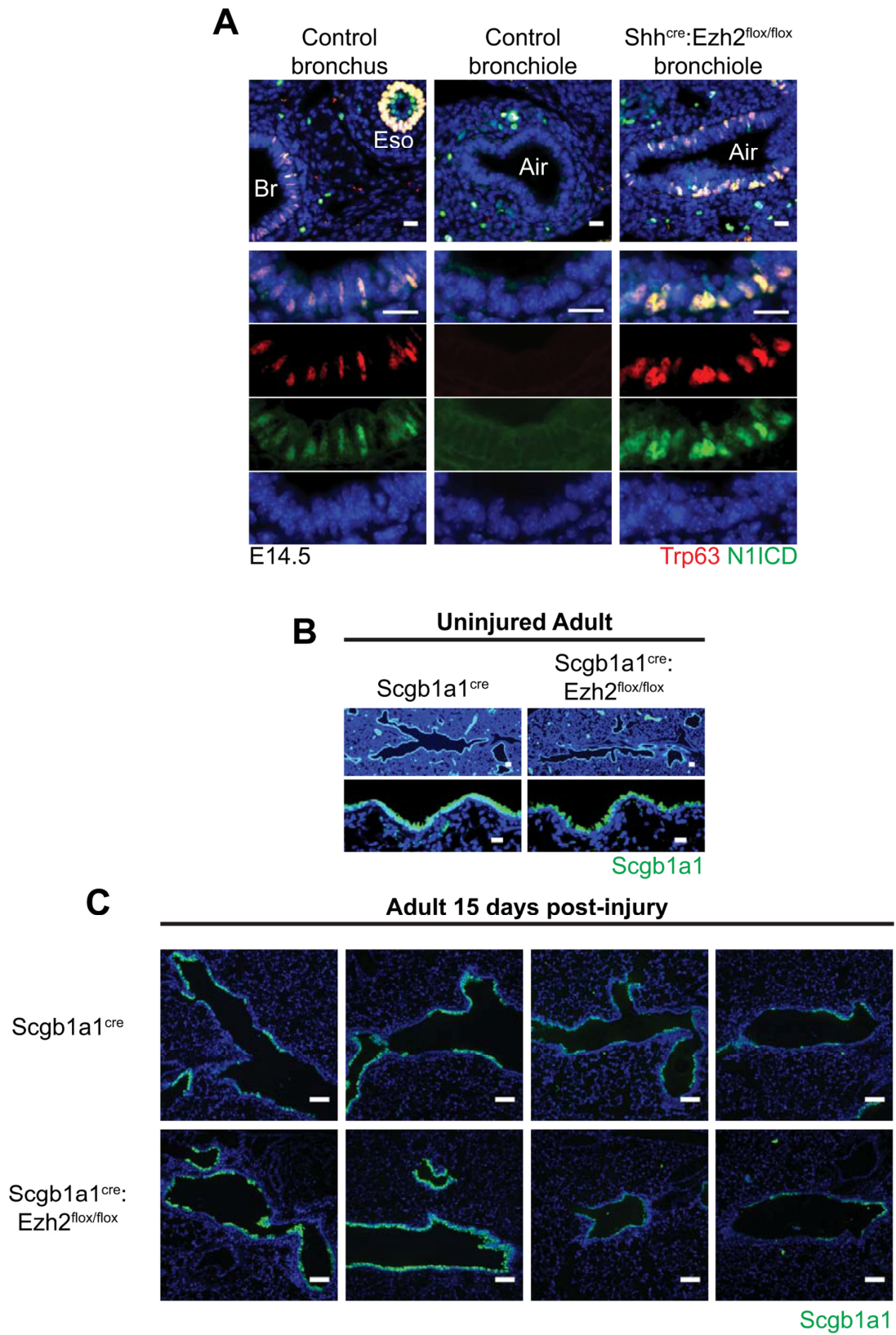


Supplemental Figure 1. Expression of Ezh2 becomes restricted during late lung development. (A) IHC for Ezh2, proximal airway epithelium marker Sox2, and distal epithelium marker Sox9 at E14.5 and E16.5. Note that Ezh2 appears in both Sox2 and Sox9-positive epithelium at these stages. (B) IHC for Ezh2 and mature proximal epithelium markers Scgb1a1 and TubbIV. Note that Ezh2 is more highly expressed in TubbIV-positive multi-ciliated cells than in Scgb1a1-positive club cells. Scale bar: E14.5 and E16.5=100µm; E16.5 inset and E18.5=20µm.



Supplemental Figure 2. Alveolar defects include de-repression of *Ezh2* target genes and altered expression of signaling pathways. (A) H+E and IHC for Sftpc and Pdnp on E18.5 control and *Shh^{cre};Ezh2^{flx/flx}* mutant lungs.

(B) qPCR for the indicated distal epithelial marker genes at E18.5. (C) Subset of gene expression changes that could be related to defects in distal epithelial differentiation in *Shh^{cre}:Ezh2^{flox/flox}* mutant lungs. (D) H+E, IHC for Sox9, and ISH for Shh and Pax2 on control and *Shh^{cre}:Ezh2^{flox/flox}* mutant lungs at E14.5. (E) Q-PCR for Sox9 and Shh at E14.5. (F) ChIP-qPCR for H3K27me3 marks on the *Pax2* promoter and an unrelated gene desert region as well as the *Gapdh* promoter at E12.5. (G) qPCR for Pax2 and Brn2 at E14.5. Scale bar: E18.5=20µm; E14.5=100µm.



Supplemental Figure 3. Ezh2 loss inhibits club cell development, but not postnatal homeostasis or regeneration. (A) IHC for Trp63 and NICD shows co-expression in the control bronchus and the *Shh^{cre}:Ezh2^{flox/flox}* mutant bronchioles, but not the control bronchiole. (B) *Scgb1a1^{cre}:Ezh2^{flox/flox}* adult mutant lungs contain normal numbers of Scgb1a1-positive secretory cells. (C) Club cell regeneration after naphthalene-induced injury is unaffected in *Scgb1a1^{cre}:Ezh2^{flox/flox}* lungs as compared to control lungs. Scale bar: (A)=20μm; (B upper row)=100μm; (B lower row)=20μm; (C)=100μm.

Table S1. Microarray data for *Ezh2* knockout

[Click here to Download Table S1](#)

Table S2. PCR primers

[Click here to Download Table S2](#)